J Mater Sci (2006) 41:5907–5914
DOI 10.1007/s10853-006-0269-3

Thermal and optical properties of $Cd_{1-x}Zn_xS$ thin films by photoacoustics

P. Raji · K. Ramachandran · C. Sanjeeviraja

Received: 21 April 2005 / Accepted: 26 October 2005 / Published online: 6 July 2006

Abstract Ternary compounds $Cd_{1-x}Zn_xS$ for various Zn concentration in thin films are synthesized by spray pyrolysis and studied by photoacoustics technique for thermal and optical properties. The thermal diffusivity as a function of the alloy composition measured by photoacoustics shows a maximum at $x = 0.6$. The optical band gap increases with zinc concentration and the continuous change indicates the formation of solid solution.

PACS 78.20.Hp · 78.20.Wc · 78.40 –q · 78.40.Fy · 78.66Hf

Introduction

$Zn_xCd_{1-x}S$ thin films have been widely used as a wide band gap window material in hetero-junction photovoltaic solar cells [1–3] and in photoconductive devices. In solar cell systems, where CdS thin films have been proved to be useful, partial substitution of Zn for Cd increases the optical window of the hetero-junction and also diffusion potential [4].

$Zn_xCd_{1-x}S$ thin films have been prepared by a variety of techniques including spray pyrolysis [5] solution growth [6], metal–organic vapor phase epitaxy (MOVPE) [7], molecular-beam epitaxy (MBE) [8] and ion-beam deposition [9].

Recently Redwan et al. [10] have synthesized $Zn_xCd_{1-x}S$ films just for $x = 0.1$ and CdS by thermal evaporation method and in both the cases hexagonal structure was observed. Here for various concentrations the films will be prepared and structures will be studied apart from thermal and optical properties.

Thermal conductivity is one of the most important properties for understanding and calculating the heat transfer process in a material [11] and the thermal properties are the most important for improvement of the performance of any thermo controlled and energy devices.

The growing interest in physical properties of thin films initiated the development of various techniques for a generally applicable, reliable and non-contact determination of thin film thermal conductivity.

Many techniques have been developed to measure thermal conductivity of materials which can be characterized into contact and non-contact methods. The contact methods, such as using thermocouples or thin film thermisters, introduce errors caused by contact resistances and, are often, time consuming in preparation of experiments [12]. Such measurements on thin films will be less accurate. So, this demands an alternate method to measure thermal conductivity in thin films. On the other hand, the non-contact techniques, such as optical techniques are generally more flexible in terms of the types of materials can be measured and require minimum sample preparation.

Photoacoustic spectroscopy is an important method for non-destructive characterization of semiconductor materials, convenient for measurement of non-radiative relaxation process and thermal parameters. The photoacoustic technique is a non-contact method that has been used

P. Raji (✉) · K. Ramachandran
School of Physics, Madurai Kamaraj University, 162 A, North Street, Uthamapalayam, Theni, Madurai 625 021 Tamilnadu, India
e-mail: rajimku@rediffmail.com

C. Sanjeeviraja
Department of Physics, Alagappa University, Karaikudi 630 003, India

successfully to measure thermal conductivity of many materials.

In this work we use photoacoustics spectroscopy (PAS) (as this method can measure the properties without contacting the sample) to obtain the thermal diffusivity, thermal conductivity and band gap of $Cd_{1-x}Zn_xS$ thin films prepared using chemical spraying method by varying the concentration of zinc in the range ($0.0 < x < 1$).

Experiment

$Cd_{1-x}Zn_xS$ thin films ($x = 0.1$–1) were prepared using spray pyrolysis, by taking 0.4 M aqueous solution of thiourea, 0.4 M aqueous solutions of $CdCl_2$ and 0.4 M of $ZnCl_2$. Different films were prepared from solutions having different mole ratios of $CdCl_2$ and $ZnCl_2$. The solutions were mixed and then sprayed onto heated substrate. The substrates were microscopic plane glass slides of area 3.5×2.5 cm and thickness 0.1 cm and they were cleaned as usual. The substrate heater was a cylindrical furnace designed indigenously. Chromel–alumel thermocouple fixed on a dummy substrate holders was used to monitor the temperature of the substrate.

The major preparatory parameters in the spray pyrolytic process are substrate temperature, the concentration and the mole ratios of starting solutions. In this present work the films were grown at air temperature, the spray rate was 18 cc/min and the distance between the spray nozzle and the substrate was 30 cm. After deposition, the films were fast cooled at room temperature. The spray time is 10 s and six times the solution is sprayed on the substrate. The thickness of the films are in the range of 2–5 μm.

Surface morphology

The surface morphology and defects were investigated by SEM and it is given in Fig. 1 for just one sample, $Cd_{0.4}Zn_{0.6}S$ film. The thickness of the thin film varies from 2 to 5 μm. The sizes of the grain were also observed in this SEM. The growth of the layers is oriented in c axis normal to the substrate. The average particle size was estimated as 25 nm for this film and other pictures indicate that the size of the particles decreased with Zn concentration. The film is otherwise uniformly, coated except few defects and this concentration is negligible compared to the host.

Structural properties

Specular and adhesive $Cd_{1-x}Zn_xS$ films were obtained throughout the composition range ($0 \le x \le 1$). As grown $Cd_{1-x}Zn_xS$ films are bright yellow orange and the yellowness increases with increasing zinc concentration. Pure ZnS films are transparent in color.

As an example, X-ray pattern for the CdS thin film is given in Fig. 2. The primary peak obtained for CdS thin film agrees with the ASTM standard, thus demonstrating the crystallinity of the film.

ZnS and CdS are known to exist in either the cubic (zinc blende) or hexagonal (wurtzite) crystal structure depending on the preparation conditions [13]. Analysis of the X-ray diffraction data showed that films containing up to 60% ZnS have hexagonal wurtzite structure characteristic of CdS. At 80% of ZnS, however, the structure is cubic zinc blende type characteristic of ZnS. This means that the transition from the wurtzite structure to the zinc blende form takes between 60 and 80% ZnS concentration. It was observed that the diffraction angle of (002), shifts towards higher angles with an increase in the ZnS concentration,

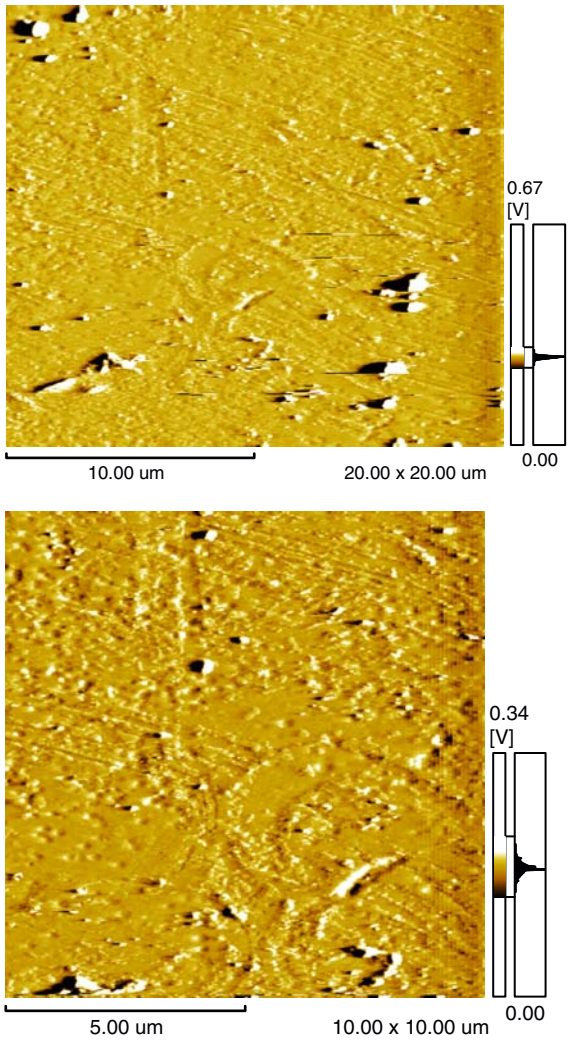

Fig. 1 SEM for $Cd_{0.4}Zn_{0.6}O$ film

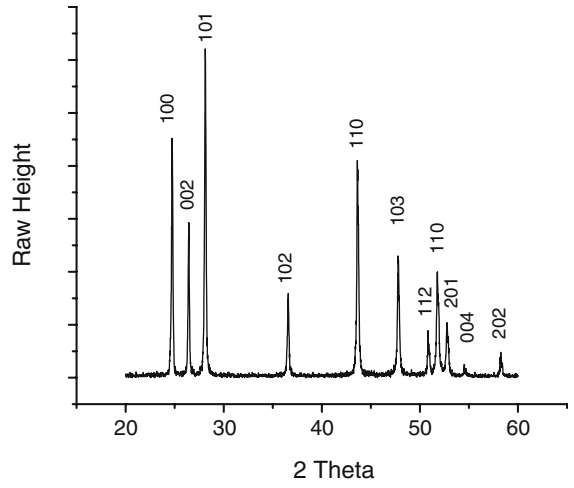

Fig. 2 X-ray diffraction pattern for Cd_1Zn_0S thin film

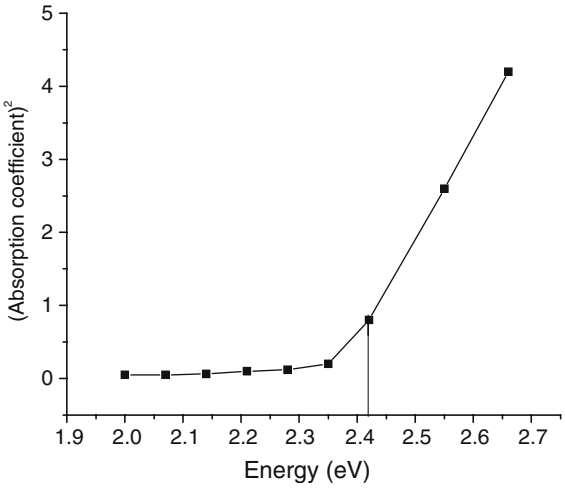

Fig. 3 Variation of α^2 with energy for Cd_1Zn_0S

which means that the (002) lattice constant decreases. At compositions where both modifications are present, the basal plane spacing is the same for the hexagonal (002) and cubic (111).

Optical properties

Optical absorbance against the wavelength is then observed for $Cd_{1-x}Zn_xS$ thin films in the wavelength range 200–900 nm with glass as the reference. The absorbance spectrum shows a sharp increase in absorption at wavelength near to the absorption edge of the threshold wavelength for onset of absorption, the energy corresponding to this determines the band gap of the semiconductor material. For example, the CdS film shows absorption coefficient (α) of about 5×10^4 cm^{-1} near the absorption edge. This shows that the deposited semiconductor film is a direct band gap material [14]. For allowed transition $(\alpha)^2$ is plotted against energy ($E=h\gamma$) to yield a straight line for direct transitions as shown in Fig. 3 from which the band gap is found to be 2.41 eV.

Photoacoustics

When a modulated light is absorbed by the sample located in a sealed cell, the non-radiative decay of the absorbed light produces a modulated transfer of heat to the surface of the sample. This modulated thermal gradient produces pressure waves in the gas inside the cell that can be detected by the microphone attached to the cell. The resulting signal depends not only on the amount of heat generated in the sample (and, hence, on the optical absorption coefficient and the light-into-heat conversion efficiency of the sample) but also on how the heat diffuses through the sample [15]. The quantity, which measures the rate of heat diffusion in a material, is the thermal diffusivity α which is a unique parameter.

Photoacoustic spectrometer

A 400 W Xe- lamp (Jobin Yvon) is mechanically chopped by an electro-mechanical chopper (Model number PAR 650) and focused onto the sample through a monochromator (Model Triax 180, Jobin Yvon). The sample is placed in the PA cell and the mike is placed very near to the sample and the PA cell is non-resonant type and made up of stainless steel. The PA signal from the microphone is fed to a lock in amplifier (Model Perkin Elmer 7225 DSP). The PA experimental setup is shown in Fig. 4.

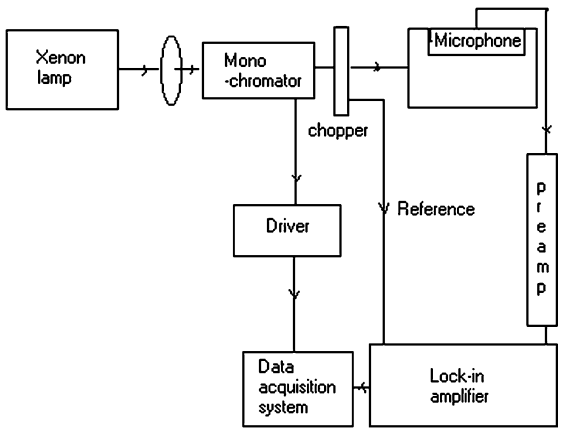

Fig. 4 Photoacoustic spectrometer

Photoacoustic measurements

Since, whatever the PA measurements made on this sample, this would give only the effective value of glass substrate and the $Cd_{1-x}Zn_xS$ film. Since the thermal diffusivity measured will be an effective value as the thin film deposited on a glass or any substrate should be treated as a two-layer system, the effective thermal diffusivity will be given in terms of the thermal diffusivities of the constituent layers.

The validity of the two-layer model was analysed in detail by Alvarado-Gil et al. [16] when they measured the thermal diffusivity and thermal conductivity for CdTe thin films which are grown by the close vapor transport technique on glass by photoacoustic technique. When they deposited the film on a glass substrate of thickness 0.1 cm, a film thickness of about 55 μm will be alright to follow two-layer model.

The approach is based on the heat diffusion equation. The starting point is the observation that the thermal diffusivity can be defined by the relative change in the amplitude of a thermal wave in semi infinite media. They found the solution of the one dimensional heat conduction equation without initial conditions but including a boundary conditions. The effective thermal diffusivity depends on relative thickness of materials, thermal diffusivities of each layer and the ratio of thermal conductivities of materials.

The thermal diffusivity of the two layer system is,

$$\alpha = \frac{1}{\frac{x^2}{\alpha_1} + \frac{(1-x)^2}{\alpha_2} + x(1-x)\left(\frac{\lambda}{\alpha_1} + \frac{1}{\lambda\alpha_2}\right)} \tag{1}$$

where $x = \frac{l_1}{l}$ is the thickness fraction of material 1 in the composite sample, and $\lambda = \frac{\kappa_1}{\kappa_2}$.

Tominaga and Ito [17] have shown the effective thermal diffusivity for a two layer model as

$$\frac{l}{\sqrt{\alpha}} = \frac{l_1}{\sqrt{\alpha_1}} + \frac{l_2}{\sqrt{\alpha_2}} \tag{2}$$

where l_1 and l_2 are the thickness of glass and sample and α_1 and α_2 are their thermal diffusivities, respectively. However it has been showed that this approach is not in agreement with the experimental data [18].

Considering the limiting case, corresponding to thermally thin material $\left[\sqrt{\frac{\omega}{2}}\right]\frac{l_1}{a_1} << 1$ ($\omega = 2\pi f$). (f is chopping frequency).

The effective thermal conductivity is given as,

$$\frac{l}{\kappa} = \frac{l_1}{\kappa_1} + \frac{l_2}{\kappa_2} \tag{3}$$

where κ_1 and κ_2 are thermal conductivities of glass and sample respectively.

(a) Depth profile analysis

The experimental measurements are done as follows.

The depth profile analysis by PA is carried out for two cases;

(i) glass plate deposited with the film
(ii) glass plate alone

i.e. firstly the glass plate with the thin film coated is taken inside the PA cell and the PA signal is observed for different chopping frequencies. This is given in Fig. 5 for just one sample as an example. As the chopping frequency is varied, the length through which the thermal energy penetrates into the sample varies. Thermal diffusion length (l_c) is a characteristic property of any system and supposed to be unique and beyond which the thermal energy cannot diffuse. For example, if a sample of thickness l is taken for measurements in PA, the Eq. 3 is valid only for thermally thin sample. i.e. $l < l_c$. For $l > l_c$, when the sample thickness is more compared to the thermal diffusion length, then this Eq. 3 cannot be used to evaluate the thermal properties. This is a case of thermally thick sample. Characteristic frequency f_c is again a unique property, as long as $l < l_c$, as can be seen from Eq. 3. The sample is thermally thick for $f > f_c$ and thermally thin for $f < f_c$. At $f = f_c$, there is a cross over from a thermally thick to a thermally thin regime, f_c is estimated from Fig. 5 (f_c corresponds to the frequency, at which a change in slope is observed in the Fig. 5).

If f_c is the characteristic frequency of the sample of thickness 'l', then the thermal diffusivity can be calculated from,

$$D = f_c l^2\, m^2\, s^{-1} \tag{4}$$

Thermal conductivity is,

$$\kappa = D\rho C_p\, \mathrm{Wm^{-1}\,K^{-1}} \tag{5}$$

where ρ is the density and C_p is the specific heat capacity of the sample. The density and specific heat are calculated from the Vegard's law for the bulk ZnS and CdS and as a first approximation this value is used for thin film.

Such measurements are done for the other $Cd_{1-x}Zn_xS$ thin films also. Now for the glass plate alone as the sample, the PA measurements were done and with these two sets of data on thermal diffusivity of the glass plate and the effective thermal diffusivity of glass plate and the film, thermal diffusivity for the film alone is computed from

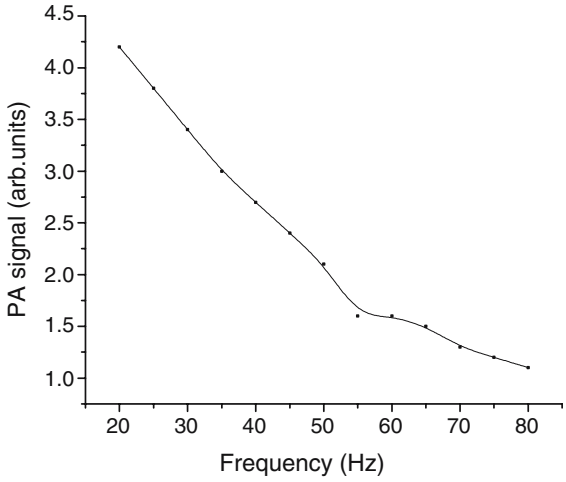

Fig. 5 Depth profile analysis for the $Cd_{0.4}Zn_{0.6}S$ alloy

Eq. 1. The measured thermal diffusivity of the glass thus here is 5.13×10^{-7} m^2/s which compares well with the literature value 5.1×10^{-7} m^2/s [19]. So, the diffusivities of the various $Cd_{1-x}Zn_xS$ thin films thus are measured and given in Table 1.

(b) Photoacoustic spectrum

Photoacoustic power detected will be proportional to the absorption of the optical energy by the sample. The PA spectrum for the $Cd_{1-x}Zn_xS$ was obtained by recording the PA signal as a function of the wavelength of the incident beam, for a constant modulation frequency. The PA spectrum for each sample is normalized using the PA spectrum obtained for carbon black. This is essential as the power spectrum of the light source (Xenon lamp) is simply the PA spectrum for photoacoustically opaque samples. Optical absorption coefficient is directly proportional to the PA signal and from the PA amplitude-wavelength plot, shown in Fig. 6, the energy gap is determined.

Non-uniformity in the size of the particles on the films would cause the additional peaks of smaller intensities. The preliminary peak, corresponding to 500 nm is taken from Fig. 6. for the calculation of band gap. The wavelength λ_g, corresponding to the peak in the PA spectrum is measured. From this, the band gap is calculated using the relation $E_0 = hc/\lambda_g$, as the present system has a direct band gap. Similarly, for the other samples, such values for the band gap are measured and given in Table 1.

Results and discussion

Thermal diffusivity of $Cd_{1-x}Zn_xS$ alloys increases as Zn concentration increases and reaches a maximum value at $x = 0.6$ and then decreases for other higher concentrations.(Here, thermal diffusivity of thin film $Cd_{1-x}Zn_xS$ alone is considered and not the glass substrate).

As it is well known the thermal conductivity of a solid is due to the heat transport by both phonons and carriers. In the case of semiconductor, the carrier concentration is generally small compared with that in a metal. The lattice contribution to the thermal conductivity of a semiconductor ($\kappa=\kappa_L+\kappa_e$) should therefore be larger than the electronic contribution. However, in doped crystals the electronic contribution may be appreciable. At $x = 0.6$, the electronic thermal conductivity decreases at the same time thermal conductivity exhibits a peak. This suggests that the peak at $x = 0.6$ may be due to kink in the lattice thermal conductivity.

Hernandez–Gueveara et al. [25] studied the optical and thermal properties of $Cd_{1-x}Zn_xS$ embedded in a zeolite host. For x values greater than 0.3, the thermal diffusivity

Table 1 Thermal properties of $Cd_{1-x}Zn_xS$ thin films at room temperature for various concentration

Concentration x	Thermal diffusivity in 10^{-10} (m^2 s^{-1})	Thermal conductivity in 10^{-4} (Wm^{-1} K^{-1})	Thermal conductivity (Wm^{-1} K^{-1}) [Bulk]	Energy gap (eV)	Energy gap [Bulk] eV	Thermal conductivity (Wm^{-1} K^{-1}) [nano CdS]
0 [CdS]	3.43	3.99	0.42 [20]	2.41	2.4 [21]	4.08 [22]
0.1	3.79	4.36		2.49		
0.2	4.16	4.73		2.56		
0.3	4.41	4.96		2.63		
0.4	4.65	5.16		2.7		
0.5	8.24	8.92		2.79		
0.6	8.82	9.68		2.84		
0.7	7.65	8.18		2.96		
0.8	7.29	7.69		3.01		
0.9	6.71	6.98		3.06		
1 [ZnS]	6.4	6.59	0.64 [23]	3.18	3.16 [24]	

(Error in the measurements ~2%)

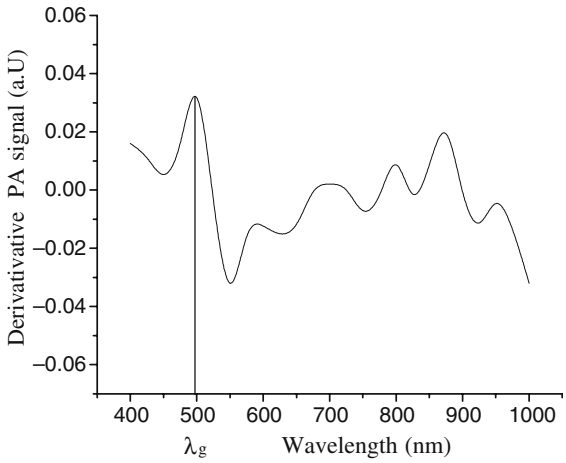

Fig. 6 PA spectrum of the sample $Cd_{0.8}Zn_{0.2}S$

and effusivity increase, and for $x = 0.6$ the thermal diffusivity reaches a maximum and then decreases.

The present PA measurements are in the line of Hernandez–Gueveara et al., and also show that the thermal properties do not depend on the substrate (as only the film property are deconvoluted) is shown in Fig.7.

Ferreira et al. [26] have studied the thermal diffusivity of $Pb_{1-x}Sn_xTe$ alloys by photoacoustic measurements. The behavior of α is, upto $x = 0.12$, the thermal diffusivity tends to decrease, except for an initial kink at $x = 0.02$. Above $x = 0.12$, the thermal diffusivity exhibits a peak at $x = 0.2$.

Ghosh et al. [27] have studied the thermal properties of $ZnSe_xTe_{1-x}$ alloys. The thermal diffusivity obtained as a function of concentration is found to vary non-linearly with concentration with a minimum around $x = 0.48$ and then increases to a maximum value for ZnSe.

There are many experimental reports available to justify the reduction (upto 50%) in thermal conductivity in semiconductor thin films than bulk. [28–31]. This is basically

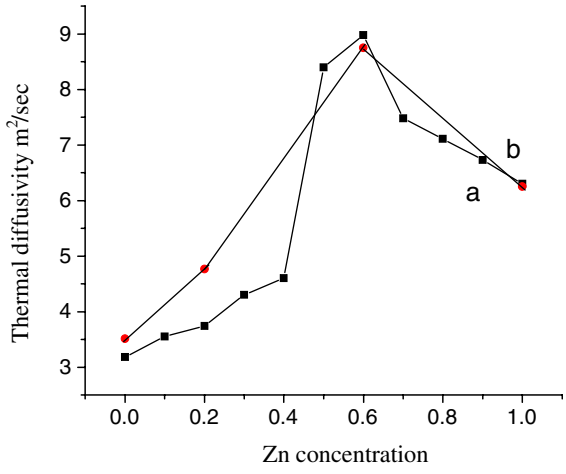

Fig. 7 Effective thermal diffusivity values a: our results; b: Hernandez-Guevara results

due to the phonon mean free path i.e. when the film thickness is of the order of the phonon mean free path scattering is bound to occur which would reduce the thermal conductivity.

Mohamed et al. [32] have studied the thermal diffusivity of $CuInSe_2$ thin films (for different Cu/In ratios), prepared by flash evaporation by photothermal deflection technique. The thermal diffusivity is less in thin films in comparison with bulk. This is of the order of 10^{-3} times the value of bulk.

Our earlier works on nano CdS [22] show higher value for thermal diffusivity compared to bulk CdS and it is known that the thermal properties of nano systems depend very much on the number of nano particles and their shape. So the present results of thin film are not compared directly with these. But here the thermal diffusivity is small compared to the bulk values. The present measurements on thermal conductivity of $Cd_{1-x}Zn_xS$ thin films agree with the earlier results of Hernandez et al. and also that they are less than the bulk values of the end members as reported by Mohamed et al. [28]. Figure 5 showing a peak at about 0.6 for thermal conductivity and the decrease afterwards indicates clearly multiple scattering by the additive atoms. This would happen in any mixed system but generally for bulk. For example, even $KCl_{1-x}Br_x$ shows a peak at about $x = 0.24$ for Debye temperature. The phonon spectrum is modified when the proportion mixing is increasing and at time when the critical concentration is reached, scattering reduces the thermal conductivity and this bulk behaviour is reflected in this thin film also.

Fathallah et al. [33], as early as in 1987, had carried out measurements on $Cd_{1-x}Zn_xS$ thin films for typical x values of 0.09, 0.17 and 0.4 by photothermal deflection spectroscopy as this technique is less sensitive to light scattering by surface roughness and inhomogenities. The band gaps measured from this technique for these x are 2.425, 2.51 and 2.71 eV respectively. Our measurements agree fairly well with these results. Since Fathallah et al. have concentrated the region below the fundamental gap, the complete behavior was not understood. But Hernandez et al. have studied almost for all the concentrations on a zeolite host when at $x = 0.6$ a maximum in thermal diffusivity. Similarly other substrates were Na-YZ-H [34]. Similarly Dona and Herrero [35] have reported that at $x = 0.6$, there is a maximum in thermal properties in $Cd_{1-x}Zn_xS$ systems.

The reason may be viewed as follows. Even though $Cd_{1-x}Zn_xS$ forms a solid solution (from CdS to ZnS) which was observed by the band gap measurements, between 2.4 and 3.2 eV, when we assume CdS as the host system, as Zn concentration becomes larger and larger, the defect concentration becomes larger.

From the band gap, one can find the size of the particles collected on the surface of the film from

$$E_{gn} = \left[E_{gb}^2 + \left\{ \frac{2\hbar^2 E_{gb} \left(\frac{\pi}{R}\right)^2}{m^*} \right\} \right]^{1/2} \quad (6)$$

This equation is a well known and successful expression to explain the size of the particles down to about 3 nm and is derived explicitly by Wang et al. [36] following a molecular orbital theory and effective mass approximation, when they studied how small particles that contain a few several thousand atoms are critical in the evolution of molecules. They have first studied the size of the particle by X-ray diffraction for PbS particles. Scherrer's equation was used to find the size, involving the half width of the diffraction spectrum. The agreement with Eq. 6 was so good that the researchers started using this Eq. 6 for the size of the particle after Wang et al.

But the restriction is that this expression is valid only upto a size of 2.5 nm. As the semiconductor particle size decreases, in principle the band gap can move to different points of the brillouin zone due to the differences in effective masses of various bands, but it is generally believed that there is not happening here since all the other bands near the gap are separated by more than 2.4 eV, seen from the band structure of CdS i.e. the band gap is observed to depend on conduction band and valence band in the direct band gap materials.

The band gap of the $Cd_{1-x}Zn_xS$ thin films is already measured from the photoacoustic spectrum. From photoacoustic measurements, we found the size of the particle to be from 13 to 31 nm. Non-uniformity in the size of the particles in thin films, even though they are in few nm and the possible defects in the preparation of the film will also contribute to the reduction in thermal conductivity. This is first scanned by photoacoustic spectroscopy (in the form of photoacoustic microscopy). As expected for thin films, the photoacoustic spectrum showed many number of peaks indicating the presence of defects when scanned through the surface of the films.

Almost in all samples, the sizes are of the order of 13–31 nm, equivalent to the nano systems. But the thermal properties of nano CdS are quite different from this films. The reasons are evident

(i) non-uniformity in the size of the particles
(ii) defects, including voids, in large number will be present in this thin films, giving rise to additional peaks.

So the comparison of thin films with nano materials for thermal properties are not possible.

Conclusions

We have proposed photoacoustic method to determine the band gap and thermal properties of $Cd_{1-x}Zn_xS$ thin films. The thermal diffusivity reaches a maximum at $x = 0.6$. The optical band gap increases with Zinc concentration and continuous change indicates solid solution formation. It is well accepted that the four probe method is the conventional technique for such measurements. But this photoacoustics is also reliable tool for the same measurements and one can directly measure the thermal diffusivity and also band gap here.

References

1. Siu WC, Kwok HL (1978) J Phys D 11:669
2. Felgelson RS, N'Diage A, Yin SY, Rube RH (1977) J Appl Phys 48:3162
3. Banerjee A, Nath P, Vankar VD, Chopra KL (1978) Phys Stat Sol (a) 46:723
4. Reddy KTR, Reddy PJ (1992) J Phys D 25:1345
5. Chynoweth TA, Bube RH (1980) J Appl Phys 51:1844
6. Padam GK, Malhotra GL, Rao SUM (1988) J Appl Phys 69:770
7. Yamaga S, Yoshikawa A, Kasai H (1990) J Cryst Growth 99:432
8. Kawahara T, Ohkawa K, Mitsuya T (1991) J Appl Phys 69:3226
9. Kuroyanagi A (1994) Thin Solid Films 249:91
10. Redwan MA, Soliman I, Aly EH, El-Shazely AA, Zayed HA (2003) J Mater Sci 38:3449
11. Incropera FP, DeWitt DP (2002) Fundamentals of heat and mass transfer. Wiley, New York
12. Wang X, Hu H, Xu X (2001) J Heat Transf 123(1):1
13. Agnihotri OP, Gupta BK (1979) Jpn J Appl Phys 18:317
14. Sze SM (1969) Physics of semiconductor devices, 2nd edn. Wiley, New York
15. Rosencwaig A, Gersho A (1976) J Appl Phys 47:54
16. Alvarado-Gil JJ, Zelaya-Angel O, Sanchez-Sinencio F (1995) Vac 46:883
17. Tominaga T, Ito A (1988) Space Appl Phys 27:2392
18. Mansanares AM, Bento AC, Vargas H, Leite NF, Miranda LCM (1990) Phys Rev B 42:447
19. McDonald FA, Wetsel GC (1978) J Appl Phys 49:2313
20. Cesar CL, Vargas H, Mendes Filho J (1983) Appl Phys Lett 43(6):555
21. Portillo-Moreno O, Lima-Lima H (2002) Superficies y Vacio 15:19
22. Raji P, Sanjeeviraja C, Ramachandran K (2004) Crys Res Tech 39
23. Aven M (1965) Appl Phys lett 7:146
24. Fahrenbruch AL (1977) J Crys Growth 39:73
25. Hernandez-Guevara A, Cruz-Orea A, Sanchez-Sinnencio F (2000) Superficies y Vacio 10:51
26. Ferreira SO, Ying An C, Bandeira IN, Miranda LCM (1989) Phys Rev B 39:7967
27. Ghosh AK, Som KK, Chatterjee S, Chaudhuri BK (1995) Phys Rev B 51(8):4842
28. Chen G, Tien CL, Wu X, Smith JS (1994) J Heat Transf 116:325
29. Ju YS, Goodson KE (1999) Appl Phys Lett 74 (2):3005
30. Chen G (1999) J Heat Transf 121:945

31. Zeng T, Chen G (2001) J Heat Transf 123:1
32. Mohamed Fadhali MA, Asha AS, Antony A, Jyotsna R, Nair KPR, Rasheed TMA, Jeyaraj MK (2003) DAE Solid state Symposium, Gwalior, p 151
33. Fathallah M, Ben Said M, Bennaceur R (1987) Phys Stat Sol (a) 99:521
34. Gutierrez-Juarez G, Zeleya-Angel O, Alvarado-Gil JJ, Vargas H, Pastore H De O, Barone JS, Hernandez-Velez M, Banos L (1996) J Chem Soc Faraday Trans 92:2651
35. Dona JM, Herrero J (1995) Thin Solid Films 268(1–2):5
36. Wang Y, Suna A, Mahler W, Kasowski R (1987) J Chem Phys 87:7315